Nonlinear Dynamics in Nanomechanical Oscillators

Stav Zaitsev, Ronen Almog, Oleg Shtempluck, and Eyal Buks

Abstract— **In the present work we investigate nonlinear dynamics in a nanomechanical doubly clamped beam made of PdAu fabricated using bulk nanomachining and e-beam lithography. The beam is driven into nonlinear regime of oscillations and the response is measured by an electron beam displacement detector. In one set of experiments we study the impact of nonlinear damping on the dynamics in the bistable regime of operation. For data analysis we introduce a nonlinear damping term to Duffing equation. The experiment shows conclusively that accounting for nonlinear damping effects is needed for correct modeling of the dynamics. In another set of experiments we study intermodulation mechanical gain near the onset of bistability . As predicted by a theoretical analysis, we find high intermodulation gain when the system is operated close to a bifurcation.**

I. Introduction

The field of micro-machining is forcing a profound redefinition of the nature and attributes of electronic devices. This technology allows fabrication of a variety of on-chip fully integrated sensors and actuators with a rapidly growing range of applications. In many cases it is highly desirable to shrink the size of mechanical elements down to the nano-scale [1], [2]. This allows increasing the speed of operation by increasing the frequencies of mechanical resonances and enhancing their sensitivity as sensors. Moreover, as devices become smaller their power consumption goes down and their cost can be significantly lower. Some key applications of NEMS technology include magnetic resonance force microscopy (MRFM) [3], [4] and mass-sensing [5]. Further miniaturization is also motivated by the quest for mesoscopic quantum effects in mechanical systems [6], [7], [8].

Nonlinear effects are of great importance for nanomechanical devices. The relatively small applied forces needed for driving a nanomechanical oscillator into a nonlinear regime is usually easily accessible. Thus, a variety of useful applications such as frequency synchronization, frequency mixing and conversion, and parametric amplification, can be implemented by applying modest driving forces. Moreover, monitoring the displacement of a nanomechanical oscillator oscillating in the linear regime may be difficult when a displacement detector with high sensitivity is not available. Thus, in many cases the nonlinear regime is the only useful regime of operation. However, to optimize the properties of NEMS devices operating in the nonlinear regime it is important to study the underlying physics.

In the present work we study damping and intermodulation gain in a nanomechanical oscillator. We find that correct modeling of the response of the system in the nonlinear regime is possible only when nonlinear damping is taken into account. Moreover, we characterized the nonlinear response by studying intermodulation, and find that high gain is achieved when operating close to a bifurcation.

This work was supported by the German Israel Foundation under grant 1-2038.1114.07, the Israel Science Foundation under grant 1380021, the Deborah Foundation and Poznanski Foundation.

The authors are with the Department of Electrical Engineering and Microelectronics Research Center, Technion, Haifa 32000, Israel (e-mail: eyal@ee.technion.ac.il).

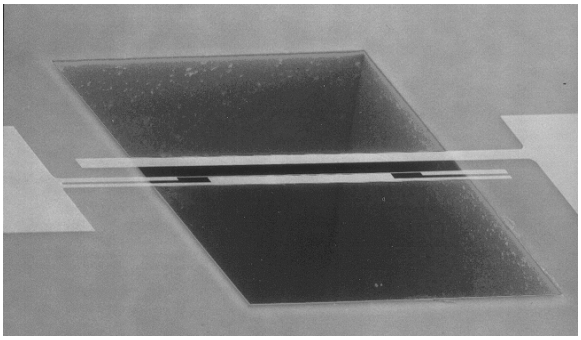

Fig. 1. The device consists of a narrow doubly clamped beam (length 200 μm, width 0.25 μm and thickness 0.2 μm) and wide electrode. The excitation force is applied as voltage between the beam and the electrode.

II. Experimental Setup

For the experiments we employ nanomechanical oscillators in the form of doubly clamped beams made of PdAu (see Fig. 1). The bulk nano-machining process used for sample fabrication is similar to the one described in [9], [10]. Measurements of mechanical properties are done *in-situ* a scanning electron microscope, where the imaging system of the microscope is employed for displacement detection [10]. A driving force is applied to the beam by applying a voltage to the nearby electrode. With a relatively modest driving force the system is driven into the regime of nonlinear oscillations [10], [11].

III. Nonlinear Damping

A key property of devices based on mechanical oscillators is the rate of damping. For example, in many cases the sensitivity of NEMS sensors is limited by thermal fluctuation which is related to damping via the fluctuation dissipation theorem. In general, a variety of different physical mechanisms can contribute to damping, including bulk and surface defects, thermoelastic damping, nonlinear coupling to other modes, phonon-electron coupling, clamping loss, etc.. Identifying experimentally the contributing mechanisms in a given system can be highly challenging, as the dependence on a variety of parameters has to be examined systematically.

Nanomechanical systems suffer from low quality factors Q relative to their macroscopic counterparts [2]. This behavior suggests that damping in nanomechanical devices is dominated by surface properties, since the relative number o

Proceedings of the 2005 International Conference on MEMS, NANO and Smart Systems (ICMENS'05)
0-7695-2398-6/05 $20.00 © 2005 IEEE

on the surface or close to the surface increases as device dimensions decrease. This point of view is also supported by some experiments [12], [13]. However, very little is currently known about the underlying physical mechanisms contributing to damping in these devices.

The effect of nonlinear damping for the case of strictly dissipative force, being proportional to the velocity to the p'th power, on the response and bifurcations of driven Duffing oscillators was studied in [14], [15]. However, for the present case we consider a Duffing oscillator having nonlinear damping force proportional to the velocity multiplied by the displacement squared (see Ref. [16]). As will be shown, this approach is equivalent to the case where damping nonlinearity proportional to the velocity cubed is considered. We have recently studied a closely related problem of a nonlinear stripline superconducting electromagnetic oscillator [17], where nonlinear damping was taken into account. With some adjustments, these preliminary results are implemented for the case of a nanomechanical nonlinear oscillator. To determine experimentally the rate of nonlinear damping, as well as the Kerr constant and other important parameters, we measure the response near the resonance in the nonlinear regime [10].

A. Equation of Motion

We excite the system close to its linear fundamental mode. Ignoring all higher modes allows us to describe the dynamics using a single degree of freedom x. First we derive the linear terms in the equation of motion and later add the nonlinear ones.

The linear equation of motion is

$$m\ddot{x} + 2b\dot{x} + kx = -\frac{d\mathcal{E}_{cap}}{dx}, \tag{1}$$

where m is the effective mass of the beam, $\mathcal{E}_{cap} = C(x)V^2/2$ is the capacitance energy, $C(x) = C_0/(1 - x/d)$ is the displacement dependent capacitance, d is the gap between the electrode and the beam, b is the damping constant, and k is the spring constant.

The applied voltage is composed of large DC and small AC components $V(t) = V_{DC} + v\cos(\omega t)$ where v is constant, $v << V_{DC}$ In our case $x << d$, and the equation of motion thus reads

$$\ddot{u} + 2\gamma\dot{u} + \omega_0^2\left[1 - \frac{2C_0 v\left[V_{DC}\cos(\omega t) + \frac{1}{4}v\cos(2\omega t)\right]}{k_e d^2}\right]u = f(t), \tag{2}$$

where $u = x - C_0V_{DC}^2/2k_ed$, $\omega_0 = \sqrt{k/m}$, $\gamma = b/m = \omega_0/2Q$ and $f(t) = C_0V_{DC}v\cos(\omega t)/dm$.

The parametric term in the above equation may play an important role in some cases. In the future we plan to fully investigate the effects resulting by such an excitation. However, in the present work we assume the parametric excitation to be far below threshold and therefore ignorable.

Next we add a nonlinear elastic term proportional to u^3 and nonlinear damping term proportional to $u^2\dot{u}$ [16]

$$\ddot{u} + 2\gamma(1 + \beta u^2)\dot{u} + \omega_0^2(1 + \kappa u^2)u = f(t). \tag{3}$$

The obtained equation of motion describes a driven Duffing oscillator having nonlinear damping.

B. Multiple Scales Approximation

We use the standard multiple scales method to solve Eq. 3, as described in [18], pp.193-208.
The following form is assumed for the excitation and the response

$$f(t) = \frac{1}{2}f_{slow}(t)e^{j\omega_0 t} + c.c., \tag{4a}$$

$$u(t) = \frac{1}{2}A(t)e^{j\omega_0 t} + c.c., \tag{4b}$$

where $f_{slow}(t)$, $A(t)$ are slowly varying envelopes (compared to the rapidly oscillating term $e^{j\omega_0 t}$). The differential equation for $A(t)$ can be shown to be

$$\omega_0\left[j\frac{dA}{dt} + j\gamma A + (j\gamma\frac{\beta}{2} + \frac{3}{8}\omega_0\kappa)A^2A^*\right] = \frac{1}{2}f_{slow}(t). \tag{5}$$

In case of simple harmonic excitation

$$f(t) = \frac{1}{2}f_0e^{j(\omega_0+\Delta\omega)t} + c.c., \tag{6a}$$

$$u(t) = \frac{1}{2}ae^{j(\omega_0+\Delta\omega)t} + c.c., \tag{6b}$$

where $\Delta\omega << \omega_0$ and f_0, a are complex constant amplitudes, the following equation can be derived from Eq. 5

$$\omega_0(j\gamma - \Delta\omega)a + \omega_0(j\gamma\frac{\beta}{2} + \frac{3}{8}\omega_0\kappa)a^2a^* = \frac{1}{2}f_0, \tag{7}$$

or by taking the modulus squared

$$\omega_0^2(\gamma^2\frac{\beta^2}{4} + \frac{9}{64}\omega_0^2\kappa^2)|a|^6 + \omega_0^2(\gamma^2\beta - \frac{3}{4}\Delta\omega\omega_0\kappa)|a|^4 + \omega_0^2(\gamma^2 + \Delta\omega^2)|a|^2 - \frac{1}{4}|f_0|^2 = 0. \tag{8}$$

Equation of the same form was obtained in [17], where a superconducting oscillator having Kerr nonlinearity in addition to nonlinear damping was considered. All subsequent analysis is thus based on [17].

When β is sufficiently small the solutions of Eq. 8 behave very much like the ordinary Duffing equation solutions to which Eq. 3 reduces to when $\beta = 0$ (see Fig. 2).

Interestingly enough, equations similar to Eq. 5 and Eq. 8 arise when the damping nonlinearity is considered to be proportional to velocity cubed

$$\ddot{u} + 2\gamma(1 + \beta|\dot{u}|^2)\dot{u} + \omega_0^2(1 + \kappa u^2)u = f(t). \tag{9}$$

Substituting β by $\beta\omega_0^2$ in Eq. 5 and Eq. 8 gives the correct relations for this case. Therefore, the behavior for these two cases is similar near the resonance frequency.

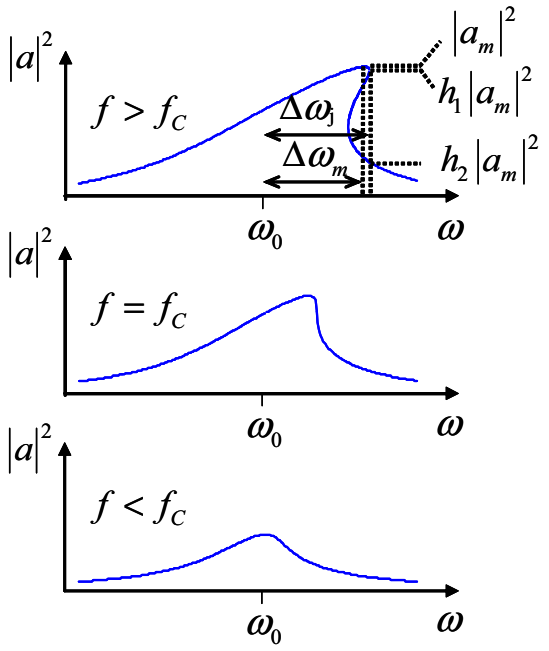

Fig. 2. Solutions of equation of motion under different excitation amplitudes f. In case $f < f_c$ only one real solution exists, no bistability is possible. In case $f = f_c$ the system is on the edge of bistability, one point exists where $|a|^2$ vs. ω has infinite slope. In case $f > f_c$ the system is in bistable regime having three real solutions over some range of frequencies. Two of these solutions are stable.

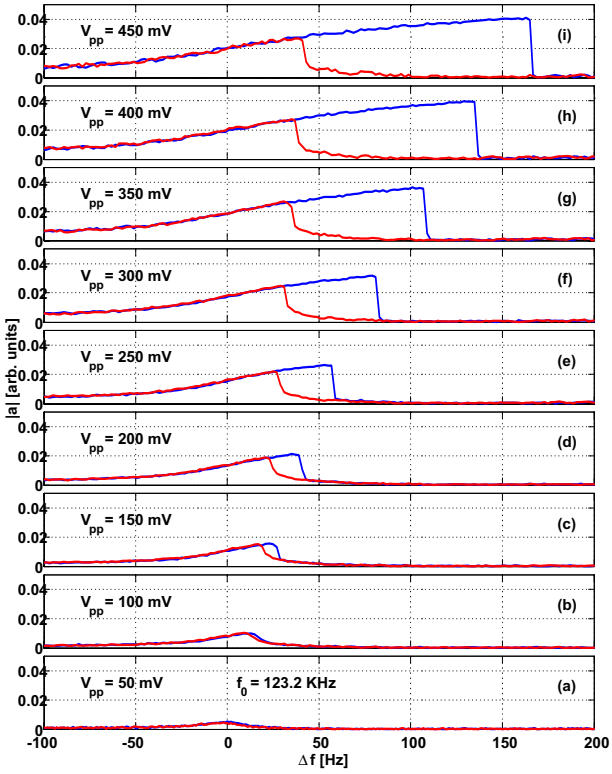

Fig. 3. Measured response vs. frequency shown for both upward and downward frequency sweeps with $V_{DC} = 20\,\mathrm{V}$ and varying peak-to-peak excitation amplitude V_{pp}.

C. Special Points

Referring to Fig. 2 we define some points in solution of Eq. 8 which we use in experimental data analysis.

The first point is the maximum response, shifted by $\Delta\omega_m$ from ω_0 and having the amplitude $|a|_m$. Differentiating Eq. 8 with respect to $\Delta\omega$ and demanding $d|a|^2/d\Delta\omega = 0$ yields

$$|a|_m^2 = \frac{8\Delta\omega_m}{3\omega_0\kappa}. \tag{10}$$

Another point of special interest is the point where the bistability jump in amplitude occurs and therefore the condition $d\Delta\omega/d|a|^2 = 0$ must be satisfied. Applying this condition to Eq. 8 yields

$$3(\gamma^2\frac{\beta^2}{4} + \frac{9}{64}\omega_0^2\kappa^2)|a|^4 + 2(\gamma^2\beta - \frac{3}{4}\Delta\omega_j\omega_0\kappa)|a|^2 + (\gamma^2 + \Delta\omega_j^2) = 0. \tag{11}$$

Equation 11 has a single real solution at the point of critical frequency $\Delta\omega_c$ and critical amplitude $|a|_c$, where the system is on the edge of bistability. This point is defined by two conditions

$$\frac{d\Delta\omega}{d|a|^2} = 0, \tag{12a}$$

$$\frac{d^2\Delta\omega}{d(|a|^2)^2} = 0. \tag{12b}$$

In general, β is positive but κ can be either positive (hard spring) or negative (soft spring). In our experiment $\kappa > 0$. By applying these conditions one finds

$$\Delta\omega_c = \frac{\gamma}{\sqrt{3}}\frac{p+3}{1-p}, \tag{13a}$$

$$|a|_c^2 = \frac{16\sqrt{3}}{9}\frac{\gamma}{\omega_0\kappa}\frac{1}{1-p}, \tag{13b}$$

where $p = 4\gamma\beta/\sqrt{3}\omega_0\kappa$. The driving force at this critical point is denoted in Fig. 2 as f_C. Note that bistable regime is accessible only when $p < 1$, namely, when the nonlinear damping β is sufficiently small in comparison with the Kerr nonlinear constant κ.

D. Experimental Data and Results

The dimensions of the beam in Fig. 1 are length 200 μm, width 0.25 μm and thickness 0.2 μm and the gap separating the beam and the electrode is 5 μm. The measured response of the fundamental mode occurring at $\omega_0/2\pi = 123.2$ kHz measured with $V_{DC} = 20\,\mathrm{V}$ and varying excitation amplitudes is seen in Fig. 3. We derive the value of $\gamma = \omega_0/2Q$ from the linear response at low excitation amplitude and find $Q = 7200$.

Our displacement detector is highly nonlinear, introducing thus a significant distortion in the measured response. In order to minimize the resultant inaccuracies, we employ the following method to extract the nonlinear parameters.

In general, the sum of the three solutions for $|a|^2$ at any given frequency can be found from Eq. 8. This is e

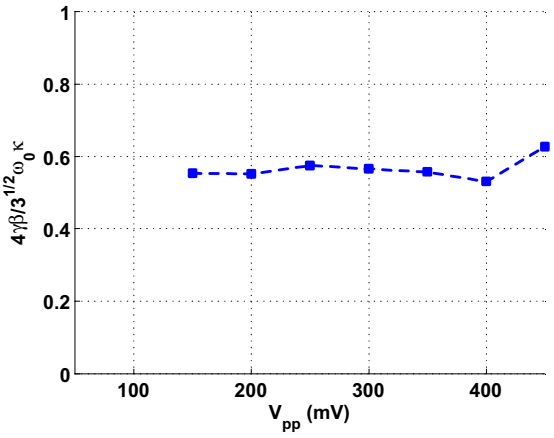

Fig. 4. Experimental results for $p = 4\gamma\beta/\sqrt{3}\omega_0\kappa$ vs. peak-to-peak excitation amplitude V_{pp} .

for the bifurcation jump point at $\omega_0 + \Delta\omega_j$ seen in Fig. 2. Using Eq. 10 to calibrate the measured response at this jump point one has

$$(2h_1 + h_2)\frac{8\Delta\omega_m}{3\omega_0\kappa} = -\frac{(\gamma^2\beta - \frac{3}{4}\Delta\omega_j\omega_0\kappa)}{(\gamma^2\frac{\beta^2}{4} + \frac{9}{64}\omega_0^2\kappa^2)}, \qquad (14a)$$

or

$$(2h_1 + h_2)8\Delta\omega_m(\frac{p^2}{3} + 1) + 16(\gamma\frac{p}{\sqrt{3}} - \Delta\omega_j) = 0, \quad (14b)$$

where h_1 and h_2 are defined in Fig. 2. Due to the frequency proximity between the maximum point and the bifurcation point at $\omega = \omega_0 + \Delta\omega_j$ the inaccuracy of such a calibration is small. Moreover, as long as excitation amplitude is high enough, h_2 is much smaller than h_1 and even considerable inaccuracy in h_2 estimation will not have any significant impact. This equation can be used to estimate p for different excitation amplitudes. The results of applying Eq. 14b to experimental data can be seen in Fig. 4.

The condition $p < 1$ is clearly satisfied and $p \approx 0.55$. Referring to Eq. 13 and Eq. 11 we see that in our system the damping nonlinearity is not negligible and has a measurable impact on both the amplitude and frequency offset of the critical point, as well as on jump points in the bistable regime. However, the underlying physical mechanisms responsible for the observed behavior remain unknown.

IV. Intermodulation Gain

Intermodulation measurement is a useful tool for characterizing nonlinearity. In this technique the oscillator in driven by a force combined of two harmonic tones having closely spaced frequencies and both laying within the bandwidth of a resonance. We refer to the tone having intense amplitude and angular frequency ω_p by the name pump, whereas to the second one having relatively small amplitude and angular frequency ω_s we refer to by the name signal. The mechanical response generated by nonlinear mixing at frequency $\omega_i = 2\omega_p - \omega_s$ is called idler.

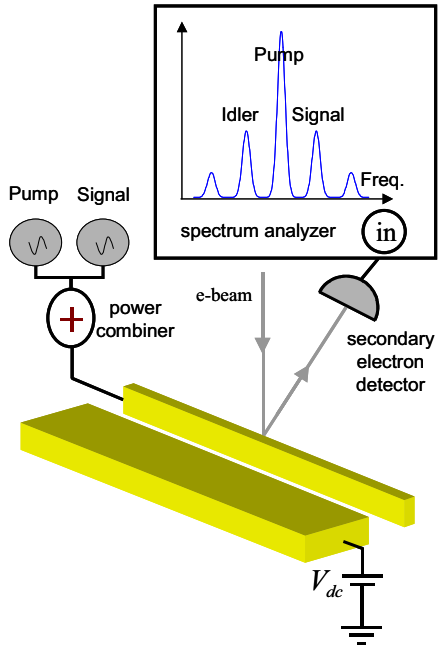

Fig. 5. Experimental setup used for the intermodulation measurements.

The response of a Duffing oscillator to such a combined drive is investigated theoretically in Ref. [17]. Linearization of the equation of motion around the point of operation of the pump yields the response of the system to small signal input. This allows calculating both, the signal gain and the idler (intermodulation) gain of the system, as a function of amplitude and frequency of the pump drive. Of particular interest is the case where the pump is tuned close to bifurcation in its nonlinear response function. In that case both calculated signal and intermodulation gains diverge in the limit of vanishing offset frequency between the signal and pump $\Delta\omega = \omega_s - \omega_p \to 0$. The actual gain of the system, which is obviously finite, depends on nonlinear terms of higher orders that come into play as soon as the amplitude of oscillation becomes appreciable. However, the divergence found in this model strongly indicates that operating close to bifurcation points is highly desirable for achieving high signal and intermodulation gains.

A. Experimental Data and Results

To study experimentally intermodulation we employ a doubly clamped beam similar to the one seen in Fig. 1, having length 100 μm, width 0.6 μm and thickness 0.15 μm, which is located adjacent to a static electrode with 4 μm gap. Figure 5 shows schematically the experimental setup. The device is biased by a DC voltage applied to the static electrode and two AC sources (pump and signal) are combined together and applied to the beam. The signal of the secondary electron detector employed as a displacement detector is analyzed using a spectrum analyzer (or a lockin amplifier).

Figure 6 shows a typical mechanical response measured with DC bias 15 V, AC pump 0.5 V and AC signal 0.05 V. As we scan the frequency forward and backward

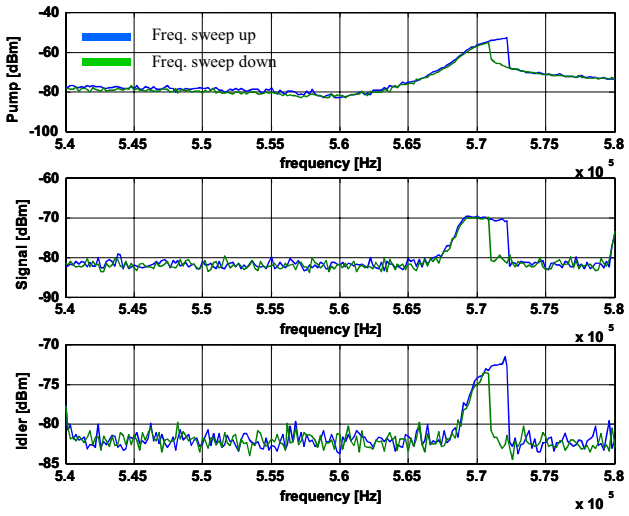

Fig. 6. Spectrum analyzer signal at pump, signal and idler frequencies measured for both, upward and downward frequency sweeps.

hysteretic response in pump, signal, and idler components for these operating parameters.

In Fig. 7 the mechanical response of pump, signal and idler is depicted as a function of both frequency and AC amplitude of the pump (The DC voltage is 15 V).

The results show a qualitative agreement with theory. As expected near bifurcation in the pump response we observe high signal and idler amplification. For both cases the gain close to bifurcation is limited by pump depletion. Further study will be devoted to analyze theoretically the behavior of the system near bifurcation. Taking into account higher order terms in the nonlinear expansion may yield a non-diverging value for the intermodulation amplification, allowing thus quantitative comparison with experiment.

V. Conclusion

In this work we demonstrate conclusively that nonlinear damping in nanomechanical doubly clamped beam oscillators may play an important role. Moreover, we study the intermodulation response of these devices and obtain high signal gain and intermodulation gain when operating near a bifurcation. However, further study is needed to investigate some important outstanding issues. For example, the underlying physical mechanisms responsible for the observed nonlinear damping are still unknown. Moreover, the intermodulation response near bifurcation requires a further theoretical study since a perturbative treatment breaks down in this limit. We hope the present work will help motivating further study in this field.

Acknowledgment

Very helpful conversations with Bernard Yurke are gratefully acknowledged.

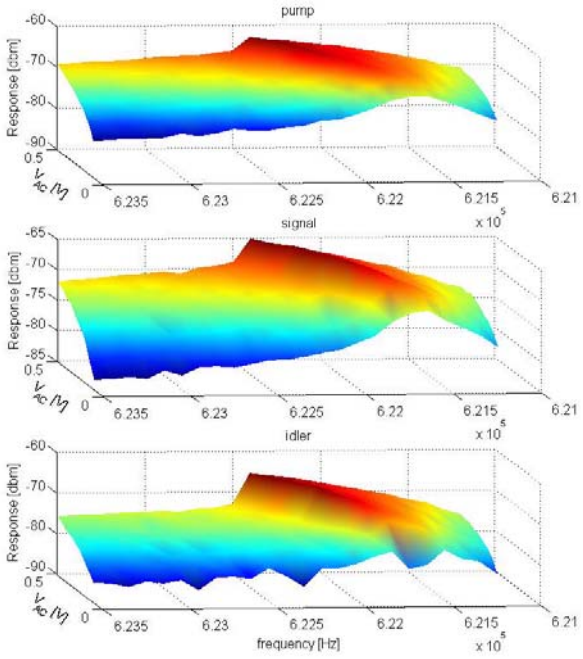

Fig. 7. Spectrum analyzer signal at pump, signal and idler frequencies vs. pump frequency and pump AC amplitude.

References

[1] M. L. Roukes, Phys. World **14**, 25 (2001).
[2] M. L. Roukes, In *Tech. Digest 2000 Solid-State Sensor and Actuator Workshop* (Cleveland: Tranducer Research Foundation); lanl e-print cond-mat/0008187.
[3] J. A. Sidles, J. L. Garbini, K. J. Bruland, D. Z. Rugar, O. Züger, S. Hoen, C. S. and Yannoni, Rev. Mod. Phys. **67**, 249 (1995).
[4] D. Rugar, R. Budakian, H. J. Mamin, and B. W. Chui, Nature **430**, 329 (2004).
[5] K. L. Ekinci, Y. T. Yang, and M. L. Roukes, J. Appl. Phys. **95**, 2682 (2004).
[6] M. Blencowe, Phys. Rep. **395**, 159 (2004).
[7] R. Knobel and A. N. Cleland, Nature **424**, 291 (2003).
[8] M. D. Lahaye, O. Buu, B. Camarota, and K. C. Schwab, Science **304**, 74 (2004).
[9] E. Buks and M. L. Roukes, Phys. Rev. B **63**, 033402 (2001).
[10] E. Buks and M. L. Roukes, EuroPhys. Lett. **54**, 220 (2001).
[11] E. Buks and M. L. Roukes, J. MEMS. **11**, 802 (2002).
[12] K. Y. Yasumura *et al.*, J. MEMS. **9**, 117 (2000).
[13] T. Ono, D. F. Wang and M. Esashi, Appl. Phys. Lett. **83**, 1950 (2003).
[14] B. Ravindra and A. K. Mallik, Phys. Rev. E **49**, 4950 (1994).
[15] Jose P. Baltanas, Jose L. Trueba, Miguel A. F. Sanjuan, Physica D **159**, 22 (2001).
[16] R. Lifshitz and M. C. Cross, Phys. Rev. B **67**, 134302 (2003).
[17] B. Yurke and E. Buks, unpublished.
[18] Nayfeh, A. H. (1981). *Introduction to Perturbation Techniques*. Wiley-Intersciences. New York.